

The expression of chirality in linked poly(thiophene)s

Birgitt Timmermans¹ | Julien De Winter² | Pascal Gerbaux² |
Guy Koeckelberghs¹ 

¹Laboratory for Polymer Synthesis, KU Leuven, Heverlee, Belgium

²Organic Synthesis and Mass Spectrometry Laboratory, Center of Innovation and Research in Materials and Polymers (CIRMAP), Mendeleiev Building, University of Mons-UMONS, Mons, Belgium

Correspondence

Guy Koeckelberghs, Laboratory for Polymer Synthesis, KU Leuven, Celestijnenlaan 200F, B-3001 Heverlee, Belgium.

Email: guy.koeckelberghs@chem.kuleuven.be

Funding information

This research was funded by Onderzoeksfonds KU Leuven/Research Fund KU Leuven. B.T. is a doctoral fellow of the Fund for Scientific Research (FWO-Vlaanderen).

Abstract

Conjugated polymers have demonstrated to express chirality, for instance, by strong circular dichroism (CD). However, the shape and intensity of the spectra can be quite different and are very difficult to predict. Molecular irregularity, star-shapes, and linking polymers have demonstrated to affect the CD, often in a positive way. In this research, we design two different chiral arms, in which the molecular irregularity results in a significantly different CD. Next, the arms are coupled to a linear core in all possible combinations. In this way, we demonstrate that rather small irregularities and linking arms to a central core increases CD, whereas heterogenous combinations result in smaller CD.

KEYWORDS

chiral expression, conjugated polymers, KCTCP, poly(thiophene)s, supramolecular organization

1 | INTRODUCTION

In the past decades, the chiral expression of conjugated polymers (CPs) has been extensively investigated. Many different backbones and chiral substituents have been employed, rendering a plethora of chiral responses.¹⁻⁷ Despite the vast amount of materials investigated, a clear relationship between the molecular structure and the chiral response remains elusive. One of the aspects in this respect is the influence of irregularities in the molecular structure. Our group has shown that small amounts of regioregularity in poly(3-alkylthiophene)s

(P3ATs) increase the strength of CD.⁸ Even variation of the location of defects affects the strength of CD.⁹ Also copolymerization¹⁰ and the nature of the end-groups can result in a much stronger response.¹¹ A similar conclusion has recently also been found in polyfluorenes: Also in these polymers, CD can increase by irregularity in the molecular structure.¹² A possible reason for the origin of the enhanced chiral response is the fact that irregularities prevent a perfect aggregate of parallel stacked polymer chains, resulting in a less organized supramolecular structure in which chiral expression is facilitated.

Abbreviations: CD, circular dichroism; CPs, conjugated polymers; Cu(I)AAC, copper(I)-catalyzed alkyne-azide cycloaddition; DBU, 1,8-diazabicycloundec-7-ene; DP, degree of polymerization; DPPA, diphenylphosphoryl azide; dppp, 1,3-bis(diphenylphosphino)propane; GRIM, Grignard metathesis; KCTCP, Kumada catalyst transfer condensative polymerization; MALDI-ToF, matrix-assisted laser desorption/ionization time-of-flight; MeOH, methanol; P3AT, poly(3-alkylthiophene); PMDTA, *N,N,N',N',N''*-pentamethyldiethylenetriamine; SEC, size exclusion chromatography; TBAF·H₂O, tetrabutylammonium fluoride trihydrate.

[This article is part of the Special issue: Chiral Materials. See the first articles for this special issue previously published in Volumes 34:12, 35:2, 35:3, 35:4 and 35:5. More special articles will be found in this issue as well as in those to come.]

Apart from linear CPs, also the chiral expression of star-shaped poly(thiophenes) was investigated. This study revealed that *perfectly regular* three-armed, star-shaped polymers exhibit a very strong and pronounced chiral expression that is much stronger than that of the individual arms that are linked to the core, which demonstrates the asset of linking chiral CPs to a central core.¹³ However, if one or two chiral arms are replaced with another (achiral) arm, and introducing irregularity in this way, the chiral response was severely diminished.¹⁴ The poor chiral response of these heterogenous star-shaped poly(thiophene)s compared with their homogeneous counterparts was attributed to the fact that the incorporated irregularity of 33% or 66% of the structure (one and two arms, respectively) is too extensive and annihilated the organization and therefore also the chiral expression.

Combined, these results indicate (i) that irregularities can facilitate a high chiral expression as long as the irregularities are not too large, in which case the supramolecular organization is complicated or even impeded and (ii) that linking CPs to a central core results in a very strong and pronounced circular dichroism (CD). It must, however, be noted that in the specific case of *star-shaped* polymers, these polymers exhibit a 2D molecular structure instead of a linear, 1D structure, which may influence the chiral response as well.

In this research, we investigate whether (i) linking chiral CPs to a central core increases CD without the necessity of a star-shape conformation and (ii) the influence of homogeneity versus heterogeneity in this system. Two different arms (**A** and **B**) are prepared together with the three possible dimers, **AA**, **BB**, and **AB**. **A** is a

homopolymer while **B** is a random copolymer composed of the enantiomer of the A-monomer and a related achiral monomer. This combination is chosen, because it has previously been shown that copolymerization can result in much stronger CD, resulting in two arms with a different CD with opposite sign.¹⁰ **AA** and **BB** are homogeneous dimers, but based on different, more specifically regular versus irregular, arms, while **AB** is a heterogeneous dimer (Figure 1).

Building on the previous studies on star-shaped CPs, (a)chiral poly(3-alkylthiophene)s equipped with an azide end-group are chosen as arms, as these CP can be reliably synthesized in a controlled way and coupled to a core containing acetylene groups.^{13,14} Two arms are linked to a phenyl ring in a 1,4-substitution pattern, providing a linear conformation instead of the star-shaped structure. Two different arms are prepared: A homopolymer, poly((*R*)-3-(3,7-dimethyloctyl)thiophene), and a copolymer, poly((*S*)-3-(3,7-dimethyloctyl)thiophene)-*random*-poly(3-octylthiophene). These polymers are synthesized using the Kumada catalyst transfer condensative polymerization (KTCTP), starting from a specific functionalized initiator. In a second step, efficient post-polymerization reactions are exploited to convert the functional group of the incorporated initiator to an azide group. In the last step, the functionalized polymer arms are coupled to ethynylbenzene or a 1,4-diethynylbenzene core via an efficient copper(I)-catalyzed alkyne-azide cycloaddition (Cu(I)AAC) click reaction.¹⁵ Note that the arms are prepared by a KCTCP, because its controlled character results in well-defined P3ATs with a controlled molar mass, a low dispersity, and a controlled end-group functionalization,^{16–21} which is of importance in the last

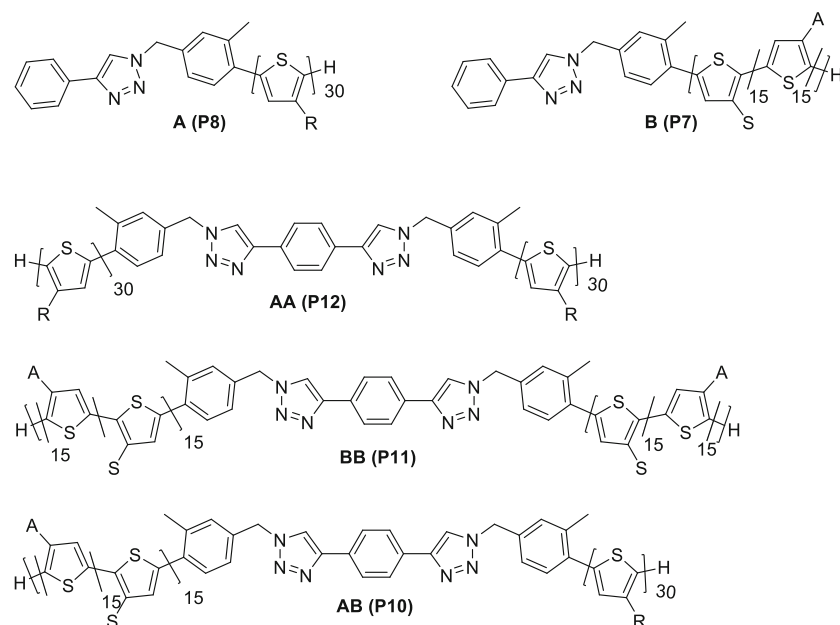
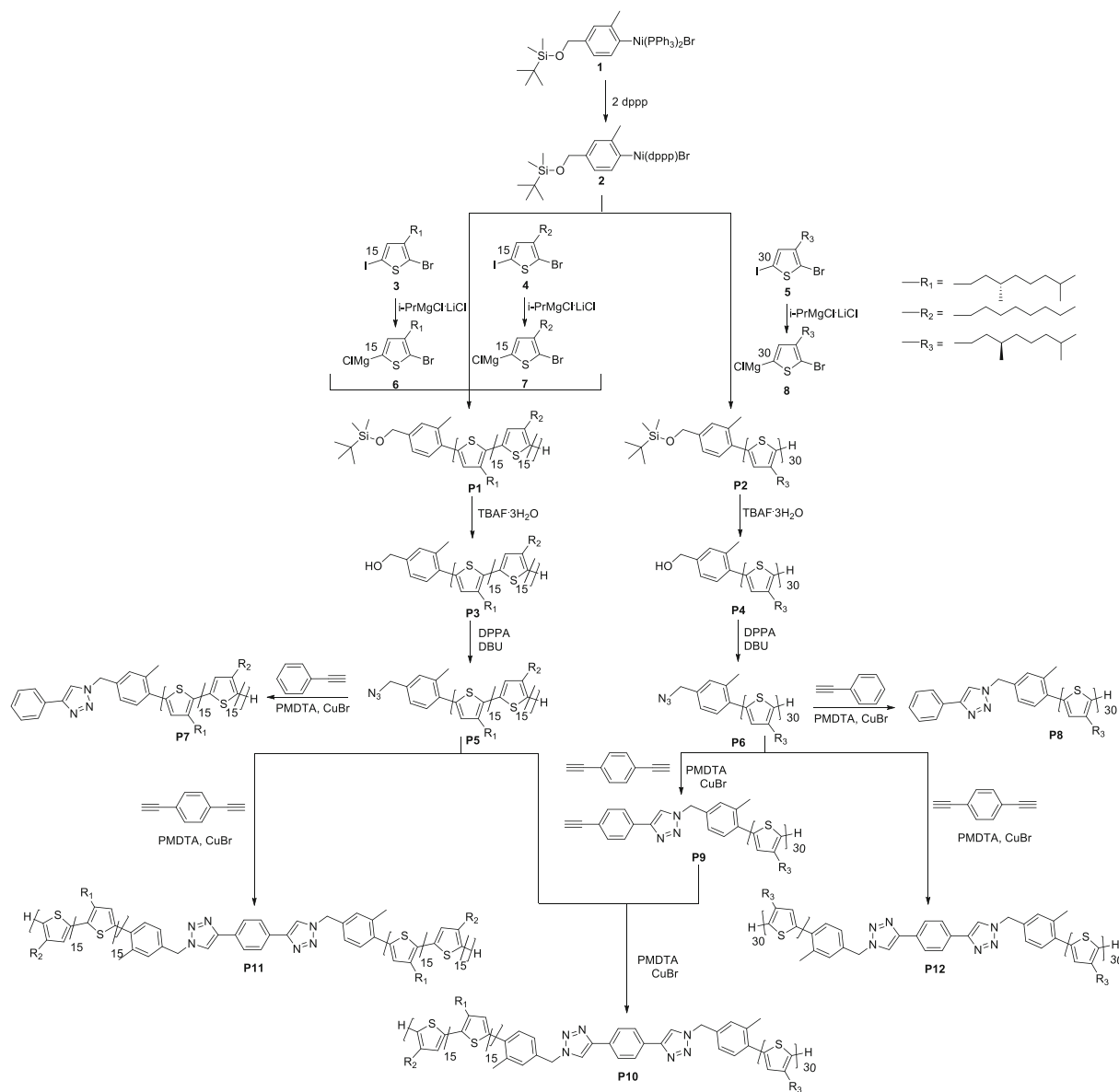


FIGURE 1 Structure of the two “arms” (**A** and **B**) and the homogeneous (**AA** and **BB**) and heterogeneous dimers (**AB**). S and R stand for the configuration of the side chain, while A is a related achiral substituent.



SCHEME 1 Schematic overview of the synthesis route of **P1–P12**.

synthesis step, as only polymer arms bearing the functional group will be coupled to the core.

2 | RESULTS AND DISCUSSION

Precursor initiator **1**²² and precursor monomers **3**,²³ **4**,¹⁰ and **5**²³ were synthesized according to literature procedures. Prior to polymerization, the precursor initiator **1** was converted in situ to the desired initiator **2** via a ligand exchange with 1,3-bis (diphenylphosphino)propane (dppp) and the precursor monomers **3**, **4**, and **5** were converted to the active monomers **6**, **7**, and **8** via a Grignard metathesis (GRIM) reaction (Scheme 1). The

polymerizations were quenched with acidified (HCl) tetrahydrofuran (1 M).

After purification by Soxhlet extraction in methanol and chloroform, polymer **P1** and **P2** were analyzed by size exclusion chromatography (SEC) to estimate the number average molar mass (M_n) and the molar mass dispersity (\mathcal{D}_M) (Table 1). The SEC elution curves can be found in the Supporting Information (Figures S1 and S2). ¹H NMR spectroscopy is performed to calculate the degree of polymerization (DP) of the polymers. A first method consists of comparing the integration of the signal of the aliphatic α -methylene protons of the monomer units to the integration of the signal of the aliphatic methyl protons of the *o*-tolyl end-group (Figure 2). For

the second method, the integration of the signal of the aromatic thiophene proton is compared with the integration of one of the signals of the aromatic protons of the *o*-tolyl end-group (Figure 2). The DP of **P1** and **P2** can only be calculated via these two methods if every polymer chain has been initiated by the *o*-tolyl initiator and if every polymer chain has an H-terminated thiophene unit, implying transfer nor termination reactions. The ^1H NMR spectra in Figure 1 show a 1:1 ratio between the integration of one of the signals of the aromatic protons

TABLE 1 Overview of the M_n , \bar{D}_M (obtained via SEC), and the DP (calculated via ^1H NMR spectroscopy).

Polymer	M_n (kg/mol) ^a	\bar{D}_M ^a	DP ^b	DP ^c
P1	9.3	1.1	30	30
P2	9.7	1.1	31	32
P3	8.4	1.1	29	31
P4	8.9	1.1	32	32
P5	8.1	1.2	31	- ^d
P6	9.2	1.1	33	- ^d

^aDetermined via SEC calibrated toward poly(styrene) standards.

^bDP calculated via ^1H NMR spectroscopy in the aliphatic region.

^cDP calculated via ^1H NMR spectroscopy in the aromatic region.

^dInaccurate due to overlapping spectra.

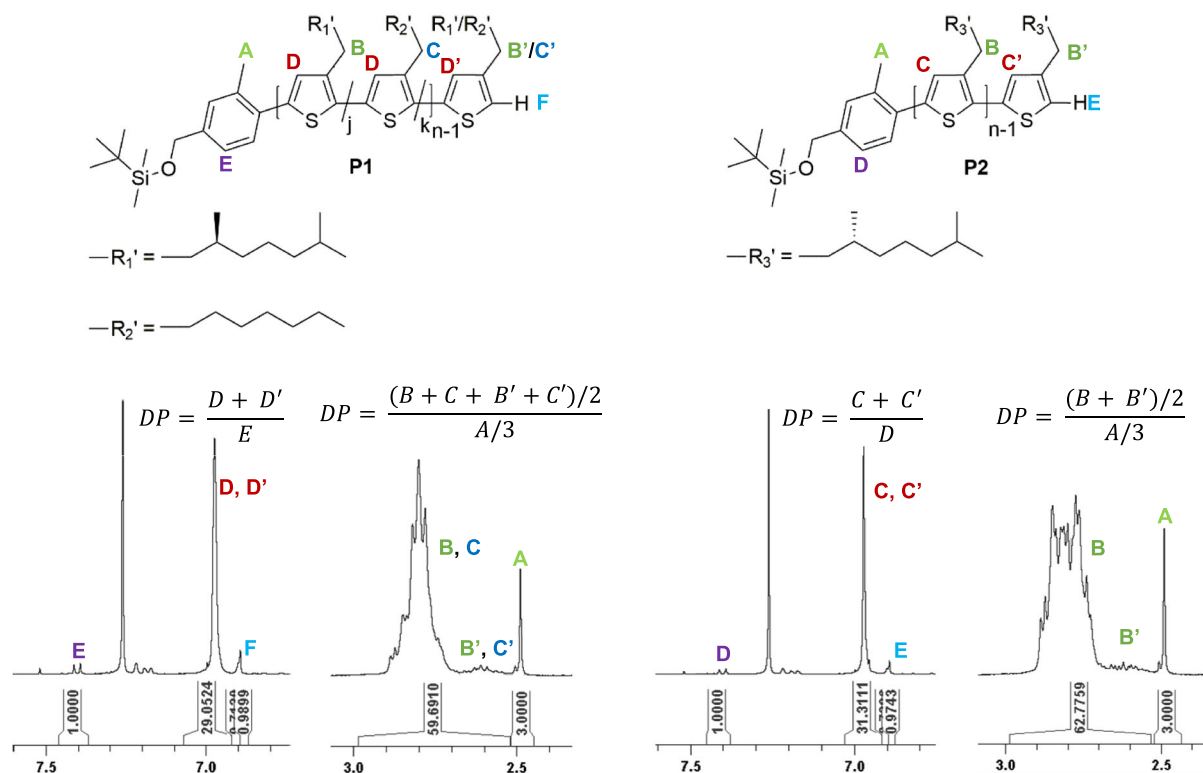


FIGURE 2 Schematic representation of the determination of the DP of **P1** and **P2** via the aromatic and aliphatic region using ^1H NMR spectroscopy.

of the *o*-tolyl unit and the H-terminated thiophene unit, indicating that every polymer chain has been initiated by the *o*-tolyl initiator and that every polymer chain has an H-terminated thiophene unit, rendering the calculations valid. Matrix-assisted laser desorption/ionization time-of-flight mass spectrometry (MALDI-ToF) further evidenced the presence of the *o*-tolyl end-group at the beginning of all polymer chains and the absence of Br-terminated polymer chains (Figures S3 and S4). Note that the DP calculated from ^1H NMR deviates from the molar mass determined by SEC. This can be explained by the fact that SEC was calibrated toward polystyrene standards, which results in an overestimation of the molar mass in case of CPs. Because also the nature of the side-chains influences the exact overestimation, no fixed relationship between both parameters is present for all polymers.

In a second step, two post-polymerization reactions were performed according to literature procedures.¹³ First, the silyl-protected alcohol functionality of **P1** and **P2** was deprotected using tetrabutylammonium fluoride trihydrate (TBAF·3H₂O), resulting in **P3** and **P4**. Then, the alcohol functionality of **P3** and **P4** was converted to an azide functionality using diphenylphosphoryl azide (DPPA) and 1,8-diazabicycloundec-7-ene (DBU), resulting in **P5** and **P6**. Both post-polymerization reactions were monitored by ^1H NMR spectroscopy to ensure full

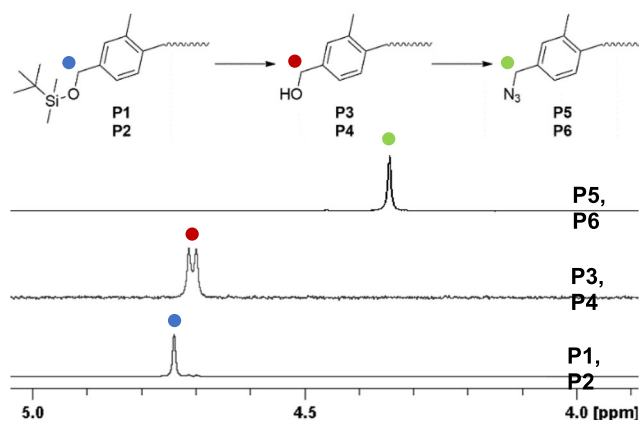


FIGURE 3 Overview of the ^1H NMR spectra of the post-polymerization reactions of **P1–P6**, indicating a small shift of the signal of the methylene protons.

conversion. A small shift of the signal of the methylene protons next to the functional group is noticed in each step (Figure 3). **P3–P6** were further analyzed via SEC to ascertain that the polymers were not negatively affected during the post-polymerization reactions (Table 1). The SEC elution curves are depicted in the supplementary information (Figures S1 and S2). MALDI-ToF measurements were performed to confirm the success of the post-polymerization reactions (Figures S3–S8).

In the last step, the functionalized polymer arms are coupled to a benzene-moiety via a Cu(I)AAC click reaction, according to literature procedures,¹³ to create the different (a)symmetric polymer systems. First, **P5** and **P6** are coupled to ethynylbenzene, using *N,N,N',N'',N'''*-pentamethyldiethylenetriamine (PMDTA) and Cu(I)Br, in order to synthesize **P7** and **P8**, respectively. A large excess of ethynylbenzene was used to ensure full conversion of the functionalized polymers. The conversion can be evaluated using ^1H NMR spectroscopy, as a clear shift of the signal of the methylene protons is noticed upon reaction (Figure 4).

Second, **P10** was synthesized in a two-step process. The first step consisted of coupling one **P6** arm to a 1,4-diethynylbenzene core to form **P9**. A large excess of core was used, to ensure that only one polymer arm was coupled to the core. This click reaction was again monitored using ^1H NMR spectroscopy to evaluate the full conversion by noticing a clear and full shift of the signal of the methylene protons next to the azide functionality (analogous to **P7** and **P8** in Figure 4). A possible side reaction in this step is the coupling of two acetylene functions, i.e. two cores, known as Glaser coupling. SEC analysis of **P9** confirmed the presence of a shoulder at double molar mass (Figure 5, black curve). **P9** was therefore purified via preparative SEC to remove the coupled

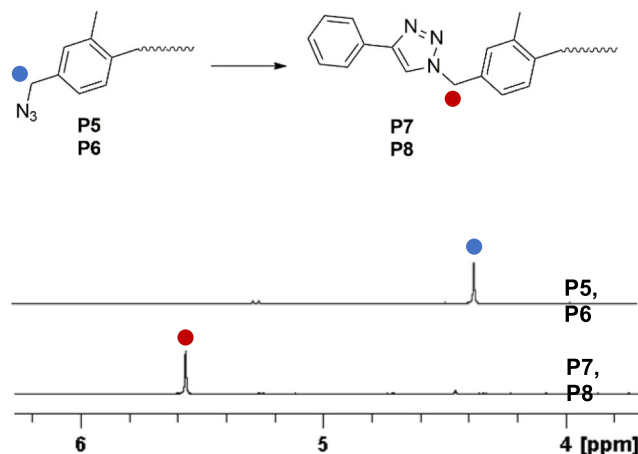


FIGURE 4 Overview of ^1H NMR spectra of the Cu(I)AAC click reaction of **P5** and **P6** with ethynylbenzene, indicating a small shift of the signal of the methylene protons.

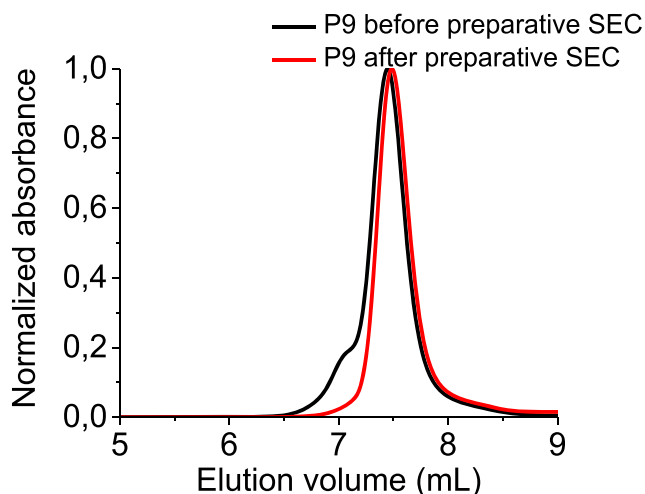


FIGURE 5 SEC elution curve of **P9** before and after preparative SEC to remove dicoupled product.

product (Figure 5, red curve). MALDI-ToF measurements were performed to check the success of the reaction and the purity of **P9** (Figure S11). In the second step of this two-step coupling, the remaining acetylene function of the core was functionalized with **P5** using again the Cu(I)AAC click reaction. This step was once more monitored using ^1H NMR spectroscopy as the signal of the acetylene proton at 3.1 ppm should disappear upon full conversion (Figure 6A). Furthermore, the ^1H NMR signals of the aromatic benzene core protons, two doublets, should converge to a singlet signal, as a symmetrical substitution of the benzene moiety is obtained (Figure 6B). In this second coupling step, an excess of **P5** was used to ensure full functionalization of the remaining acetylene functionality. The excess of the **P5** arm was removed via

TABLE 2 Overview of the M_n , D_M obtained via SEC.

Polymer	M_n (kg/mol)	D_M
P7	8.2	1.12
P8	9.0	1.2
P9	8.6	1.2
P10	20.9	1.1
P11	20.0	1.2
P12	21.6	1.1

To elucidate the chiral expression of these unique poly(thiophene) systems, solvatochromism experiments were conducted. In these experiments, nonsolvent (methanol [MeOH]) is gradually added to a solution of the polymers in a good solvent (chloroform), and a UV-vis and CD spectrum are recorded after every addition of nonsolvent. To ensure reproducibility, the nonsolvent was added at a constant speed of 0.25 mL/min via an automated syringe pump. The UV-vis and CD spectra are depicted in Figure 9.

Upon addition of nonsolvent, organization of the polymer chains is induced. Via UV-vis spectroscopy, this organization is characterized by a bathochromic shift of the absorption band and the appearance of fine structure. Furthermore, because all polymers contain chiral side chains, CD spectroscopy is used to evaluate the chiral expression of these polymers. If the polymer chains organize in a chiral way, a CD signal will appear.

First, the two polymer arms (**P7** and **P8**), coupled to a benzene moiety to better correspond to the individual arms in the coupled systems, were measured as a reference. For **P7**, which is a random copolymer of chiral and achiral units, it can be derived that the polymer chains start to organize at 33% MeOH, and a bathochromic shift can be noticed from 35% MeOH in the UV-vis spectra, which becomes more pronounced at higher percentages of MeOH (Figure 9). A fine structure in the UV-vis spectra is visible upon organization, although not strongly pronounced. The maximum of the 0–0 transition absorption band is situated at 599 nm. The appearance of a bisignate Cotton-effect at 33% MeOH indicates that the polymer chains organize in a chiral way. **P7** shows a strong chiral expression at higher MeOH content. The $g_{\text{abs, max}}$ -value ($= \Delta\epsilon/\epsilon$) is determined in order to compare the strength of the chiral expression of all the polymers in an absolute way. For **P7**, this value is $2E-2$, indicating that the strength of the chiral expression is due to a strong chiral organization of the polymer chains. For **P8**, a chiral homopolymer, organization of the polymer chains is induced at 35% MeOH, albeit very weak (Figure 9). At higher MeOH content (from 37% MeOH and up), a clear bathochromic shift can be seen,

accompanied by the appearance of a clear fine structure, indicating efficient organization. The wavelength at maximal absorbance of the 0–0 transition absorption band is 612 nm. Compared with **P7** the 0–0 transition band is more red-shifted, indicating more contribution of π - π -interactions when the polymer chains organize. The CD spectra of **P8** reveal a very weak bisignate Cotton-effect starting at 35% MeOH. At 41% MeOH, the sign of the bisignate Cotton effect switches, and a positive bisignate Cotton-effect is obtained. The $g_{\text{abs, max}}$ -value of **P8** is $3E-4$, indicating a much weaker chiral expression for **P8** compared with **P7** ($g_{\text{abs, max}} = 2E-2$). This illustrates, as previously reported, that random copolymers consisting of chiral and achiral units could exhibit a stronger chiral expression compared with their *all-chiral* counterpart.¹⁰ Furthermore, the weak chiral expression of **P8** can be explained by the more pronounced π - π -interactions, which prevent the polymer chains to stack in a chiral way.

In **P10** the random copolymer and the homopolymer are coupled to a central core. For this highly asymmetrical polymer, the polymer chains start to organize at 31% MeOH, and the bathochromic shift and the appearance of fine structure can be noticed from 33% MeOH (Figure 9). The 0–0 transition absorption band is centered around 605 nm. A weak bisignate Cotton-effect appears at 31% MeOH, indicating chiral organization. At higher MeOH content, the bisignate Cotton-effect becomes more pronounced, but switches from sign at 33% MeOH and higher, implying a change in organization upon addition of MeOH. This can be explained by the high heterogeneous character of the polymer. **P10** consists of two polymer arms with a different organization behavior. The organization of the homopolymer arm (analogous to **P8**) is largely driven by π - π -interactions, preventing a chiral organization, whereas the organization of the random copolymer arm (analogous to **P7**) is less driven by π - π -interactions, and a strong chiral organization is allowed. Furthermore, the absence of an isosbestic point in the UV-vis spectra of **P10** implies a two-step organization process, which could be caused by two competing polymer arms and which could also explain the switch in the sign of the chiral response. The combination of both arms renders **P10** highly disordered, resulting in a less pronounced chiral organization. The $g_{\text{abs, max}}$ -value of **P10** is $2E-3$, indicating a weaker chiral expression than for **P7**, but more pronounced compared with **P8**.

Afterwards, the two homo-coupled polymers **P11** and **P12** were investigated. For **P11**, which consists of two coupled random copolymers, it can be derived that organization of the polymer chains starts at 31% MeOH, as is visualized by a bathochromic shift and the appearance of fine structure (Figure 9). Furthermore, the UV-vis spectra

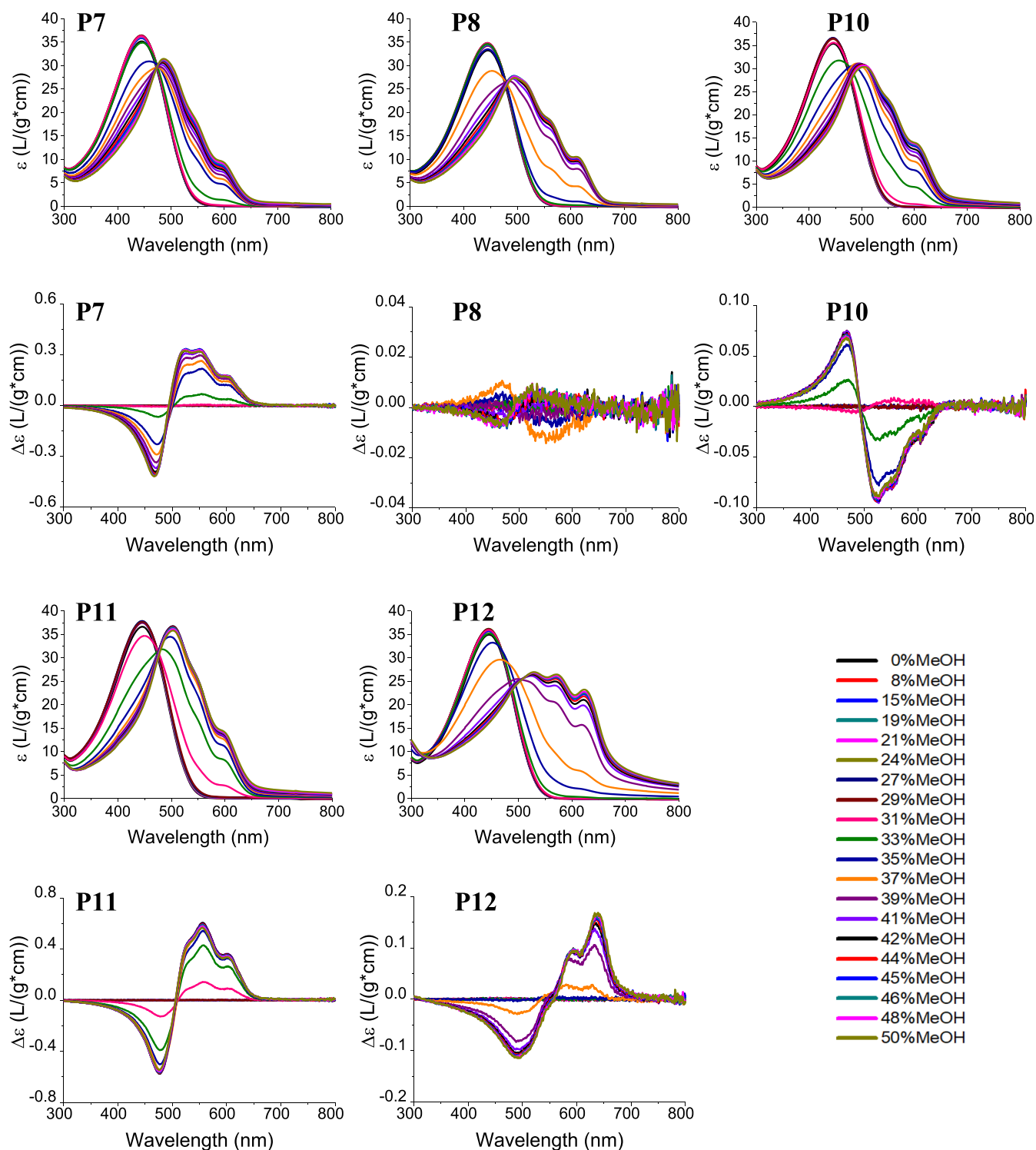


FIGURE 9 UV-vis and CD spectra of the solvatochromism experiments of **P7**, **P8**, **P10**, **P11**, and **P12**.

are characterized by an isosbestic point and the 0–0 transition absorption band is centered around 599 nm. The CD spectra of **P11** reveal a strong chiral expression, evidenced by the appearance of a strong bisignate Cotton-effect. The $g_{\text{abs, max}}$ -value of **P11** is $3\text{E}-2$, which is of the same order of magnitude as **P7**, moreover, the shape of

the CD spectra of **P7** and **P11** are quite similar, indicating a similar organization process with a pronounced chiral expression. For **P12**, the bathochromic shift and the appearance of fine structure at 35% MeOH indicate the onset of the organization of the polymer chains (Figure 9). Remarkable is the pronounced fine structure

of **P12**, which implies a strong organization of the polymer chains. The 0–0 transition absorption band has a maximum at 612 nm and is well pronounced, indicating a large contribution of π - π -interactions to the organization of **P12**. The absence of an isosbestic point indicates a two-steps organization process, which is further implied, first, by the appearance of a bisignate Cotton-effect at a higher MeOH content than at which the onset of aggregation is noticed in the UV-vis spectra and, second, by the contribution of a monosignate Cotton-effect that becomes more pronounced at higher MeOH content. The $g_{\text{abs, max}}$ -value of **P12** is $8E-3$, suggesting a stronger chiral expression for **P12** compared with **P8**. This may be unexpected because **P12** shows a pronounced fine structure and a strong 0–0 transition band, indicating an organization driven by π - π -stacking, which would lead to parallel stacks of polymer chains instead of a chiral organization. The higher chiral response for **P12** could be explained by the high symmetrical structure of the polymer, allowing long-range interactions, resulting in a long-range helical organization, explaining, nonetheless the pronounced π - π -stacking, the stronger chiral expression for **P12** compared with **P8**. We must, however, note that apart from the π - π -stacking between polymer backbones, the nonsolvent-induced aggregation process more generally depends on the interaction between the CP, solvent, and nonsolvent.^{24–26}

3 | CONCLUSION

Two linear polythiophenes with a functional group at the beginning of each polymer chain are prepared in a controlled way using KCTCP. After some postpolymerization transformations, these arms are coupled to a central core in a linear way, rendering the three possible dimers. The arms are a homopolymers and a random copolymer, which results in different CD. It is confirmed that such molecular irregularity results in stronger CD. Further, it is demonstrated that linked arms increases CD and the homogeneous dimers result in stronger CD than heterogeneous dimers.


ACKNOWLEDGMENTS

This research was funded by Onderzoeksfonds KU Leuven/Research Fund KU Leuven. B.T. is a doctoral fellow of the Fund for Scientific Research (FWO-Vlaanderen).

DATA AVAILABILITY STATEMENT

SEC elution curves, MALDI-ToF spectra and additional UV-vis and CD spectra are online available as Supporting Information free of charge.

ORCID

Guy Koeckelberghs  <https://orcid.org/0000-0003-1412-8454>

REFERENCES

- Vangheluwe M, Verbiest T, Koeckelberghs G. Influence of the substitution pattern on the chiroptical properties of regioregular poly(3-alkoxythiophene)s. *Macromolecules*. 2008;41(3):1041–1044. doi:10.1021/ma702262j
- De Cremer L, Verbiest T, Koeckelberghs G. Influence of the substituent on the chiroptical properties of poly(thieno[3,2-b]thiophene)s. *Macromolecules*. 2008;41(3):568–578. doi:10.1021/ma7024946
- Fiesel R, Halkyard CE, Rampey ME, et al. Aggregation and chiroptical behavior of a high molecular weight chirally substituted dialkylpoly(p-phenyleneethynylene). *Macromol Rapid Commun*. 1999;20(3):107–111. doi:10.1002/(SICI)1521-3927(19990301)20:33.0.CO;2-A
- Peeters E, Delmotte A, Janssen RAJ, Meijer EW. Chiroptical properties of poly{2, 5-bis[(S)-2-methylbutoxy]-1, 4-phenylene vinylene}. *Adv Mater*. 1997;9(6):493–496. doi:10.1002/adma.19970090609
- Fronk SL, Shi Y, Siefred M, Mai C-K, McDowell C, Bazan GC. Chiroptical properties of a benzotriazole–thiophene copolymer bearing chiral ethylhexyl side chains. *Macromolecules*. 2016; 49(24):9301–9308. doi:10.1021/acs.macromol.6b02229
- Oda M, Nothofer H-G, Scherf U, et al. Chiroptical properties of chiral substituted polyfluorenes. *Macromolecules*. 2002;35(18): 6792–6798. doi:10.1021/ma020630g
- Nowacki B, Zanlorenzi C, Baev A, Prasad PN, Akcelrud L. Interplay between structure and chiral properties of polyfluorene derivatives. *Polymer*. 2017;132:98–105. doi:10.1016/j.polymer.2017.07.082
- Willot P, Steverlynck J, Moerman D, Leclère P, Lazzaroni R, Koeckelberghs G. Poly(3-alkylthiophene) with tuneable regioregularity: synthesis and self-assembling properties. *Polymer Chemistry*. 2013;4(9):2662. doi:10.1039/c3py00236e
- Verheyen L, De Winter J, Gerbaux P, Koeckelberghs G. Effect of the nature and the position of defects on the chiral expression in poly(3-alkylthiophene)s. *Macromolecules*. 2019;52(22): 8587–8595. doi:10.1021/acs.macromol.9b01858
- Verswyvel M, Monnaie F, Koeckelberghs G. AB block copoly(3-alkylthiophenes): synthesis and chiroptical behavior. *Macromolecules*. 2011;44(24):9489–9498. doi:10.1021/ma2021503
- Van Den Eede M-P, Bedi A, Delabie J, De Winter J, Gerbaux P, Koeckelberghs G. The influence of the end-group on the chiral self-assembly of all-conjugated block copolymers. *Polymer Chemistry*. 2017;8(37):5666–5672. doi:10.1039/C7PY01043E
- Timmermans B, de Coene Y, Van Oosten A, Clays K, Verbiest T, Koeckelberghs G. Influence of the irregularity of the molecular structure on the chiral expression of poly(fluorene)s. *Macromolecules*. 2022;55(18):8303–8310. doi:10.1021/acs.macromol.2c00234
- Van Den Eede M-P, De Winter J, Gerbaux P, et al. Controlled synthesis and supramolecular organization of conjugated star-shaped polymers. *Macromolecules*. 2018;51(21):8689–8697. doi:10.1021/acs.macromol.8b01777
- Timmermans B, Bleus D, De Winter J, et al. Influence of heterogeneity on the chiral expression of star-shaped conjugated

- polymers. *Macromolecules*. 2020;53(21):9254-9263. doi:10.1021/acs.macromol.0c00901
15. Smeets A, Willot P, De Winter J, Gerbaux P, Verbiest T, Koeckelberghs G. End group-functionalization and synthesis of block-copolythiophenes by modified nickel initiators. *Macromolecules*. 2011;44(15):6017-6025. doi:10.1021/ma200846v
16. Yokozawa T, Yokoyama A. Chain-growth polycondensation: living polymerization nature in polycondensation and approach to condensation polymer architecture. *ChemInform*. 2004;35(2):65-83. doi:10.1002/chin.200430250
17. Yokoyama A, Miyakoshi R, Yokozawa T. Chain-growth polymerization for poly(3-hexylthiophene) with a defined molecular weight and a low polydispersity. *Macromolecules*. 2004;37(4):1169-1171. doi:10.1021/ma035396o
18. Iovu MC, Sheina EE, Gil RR, McCullough RD. Experimental evidence for the quasi-“living” nature of the Grignard metathesis method for the synthesis of regioregular poly(3-alkylthiophenes). *Macromolecules*. 2005;38(21):8649-8656. doi:10.1021/ma051122k
19. Grisorio R, Suranna GP. Intramolecular catalyst transfer polymerisation of conjugated monomers: from lessons learned to future challenges. *Polymer Chemistry*. 2015;6(45):7781-7795. doi:10.1039/C5PY01042J
20. Yokozawa T, Ohta Y. Transformation of step-growth polymerization into living chain-growth polymerization. *Chem Rev*. 2016;116(4):1950-1968. doi:10.1021/acs.chemrev.5b00393
21. Bryan ZJ, McNeil AJ. Conjugated polymer synthesis via catalyst-transfer polycondensation (CTP): mechanism, scope, and applications. *Macromolecules*. 2013;46(21):8395-8405. doi:10.1021/ma401314x
22. Smeets A, Van den Bergh K, De Winter J, Gerbaux P, Verbiest T, Koeckelberghs G. Incorporation of different end groups in conjugated polymers using functional nickel initiators. *Macromolecules*. 2009;42(20):7638-7641. doi:10.1021/ma901888h
23. Van den Bergh K, Cosemans I, Verbiest T, Koeckelberghs G. Expression of supramolecular chirality in block copoly(thiophene)s. *Macromolecules*. 2010;43(8):3794-3800. doi:10.1021/ma100266b
24. Resta C, di Pietro S, Majerić Elenkov M, Hamersak Z, Pescitelli G, di Bari L. Consequences of chirality on the aggregation behavior of poly[2-methoxy-5-(2'-ethylhexyloxy)-p-phenylenevinylene] (MEH-PPV). *Macromolecules*. 2014;47(15):4847-4850. doi:10.1021/ma500921w
25. Hassan Omar O, Falcone M, Operamolla A, Albano G. Impact of chirality on the aggregation modes of L-phenylalanine- and d-glucose-decorated phenylene-thiophene oligomers. *New J Chem*. 2021;45(27):12016-12023. doi:10.1039/d1nj02125g
26. Xue S, Xing P, Zhang J, Zeng Y, Zhao Y. Diverse role of solvents in controlling supramolecular chirality. *Chem a Eur J*. 2019;25(31):7426-7437. doi:10.1002/chem.201900714

SUPPORTING INFORMATION

Additional supporting information can be found online in the Supporting Information section at the end of this article.

How to cite this article: Timmermans B, De Winter J, Gerbaux P, Koeckelberghs G. The expression of chirality in linked poly(thiophene)s. *Chirality*. 2023;35(6):355-364. doi:10.1002/chir.23548